ELECTRON ENERGY LOSS

- STAR Time-Projection Chamber (TPC):

10% Methan / 90% Argon (2mbar above athm. pressure)

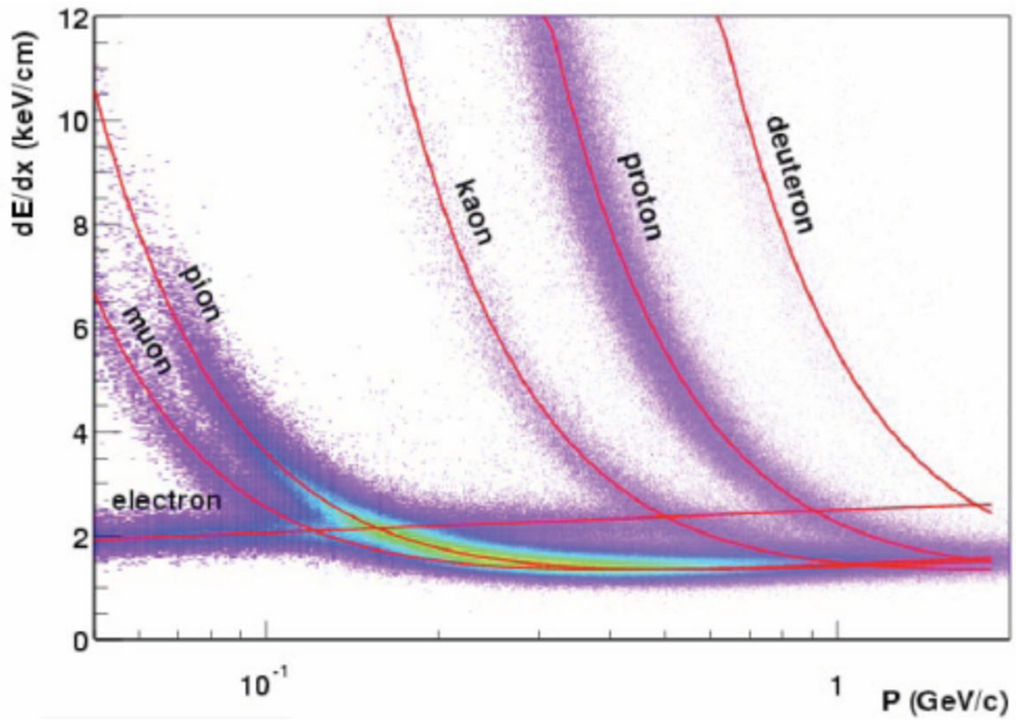

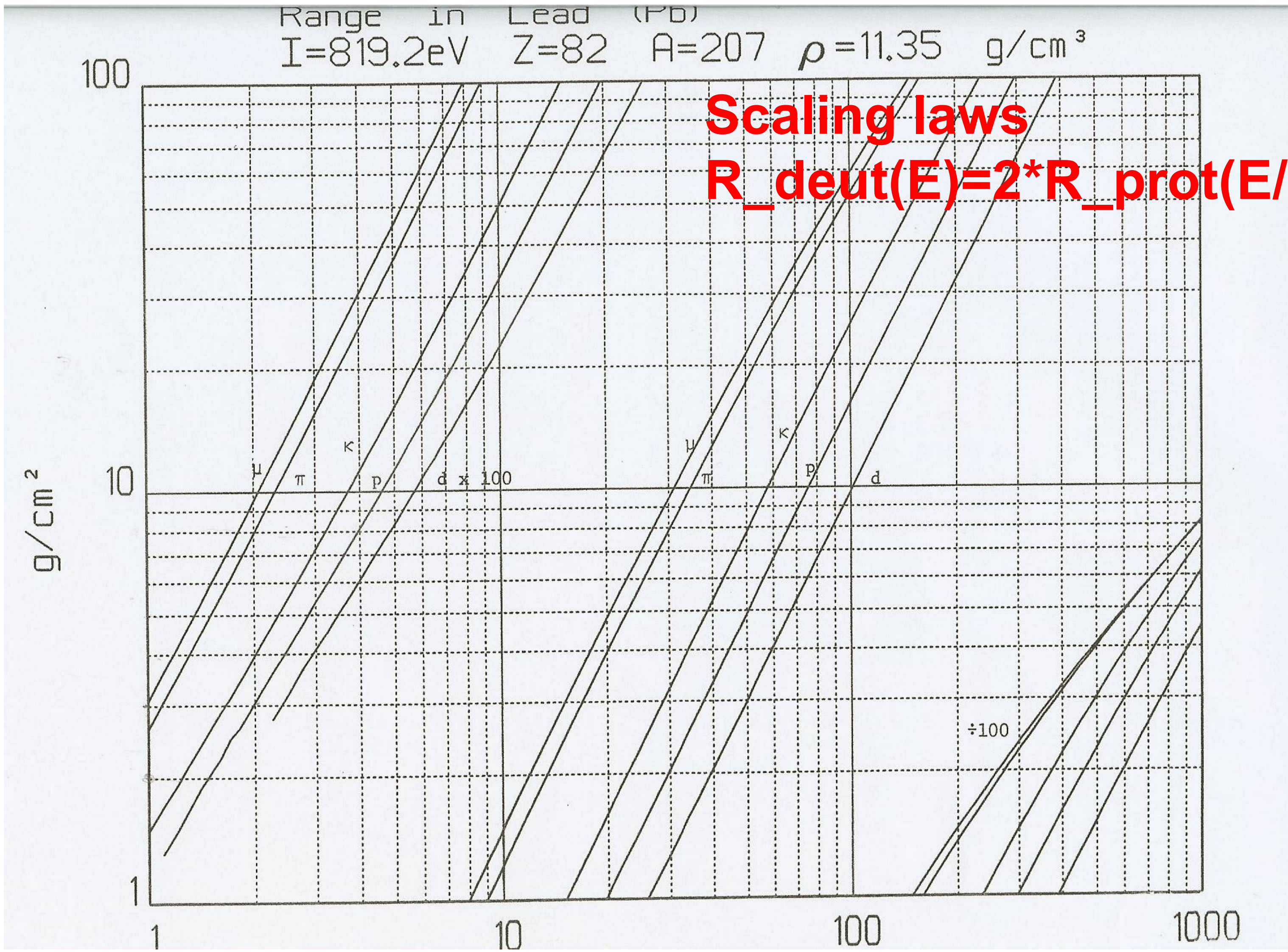

Range in Lead (Pb)
I=819.2eV Z=82 A=207 ρ=11.35 g/cm³
g/cm²
μ
π
κ
p
d x 100
÷100
1
10
100
1000
Scaling laws
R_deut(E)=2*R_prot(E/2)

Mass discrimination also possible by making RANGE measurements

See exercise n. 7 on range discrimination

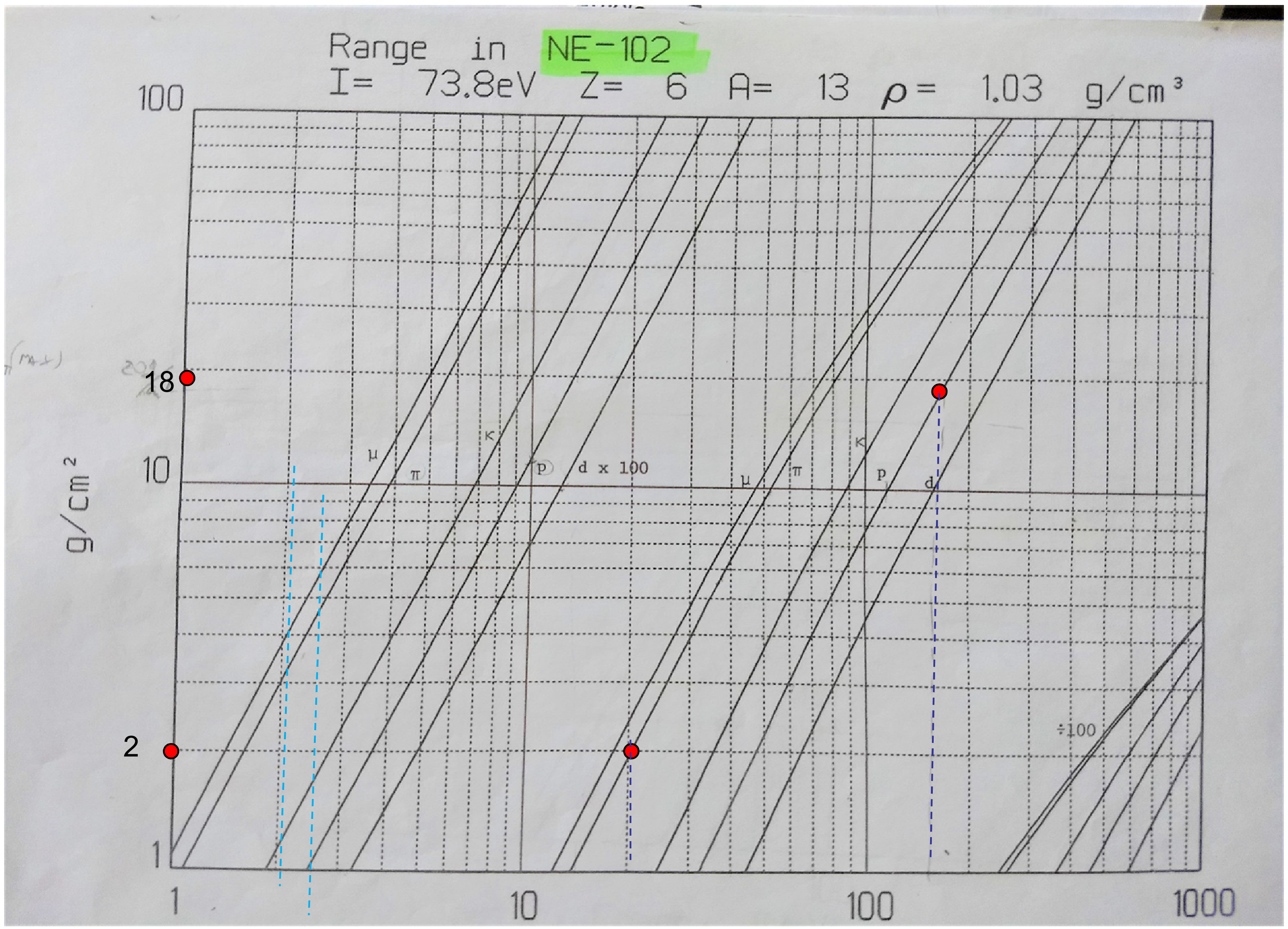

Exercise on energy loss inside/outside tumor

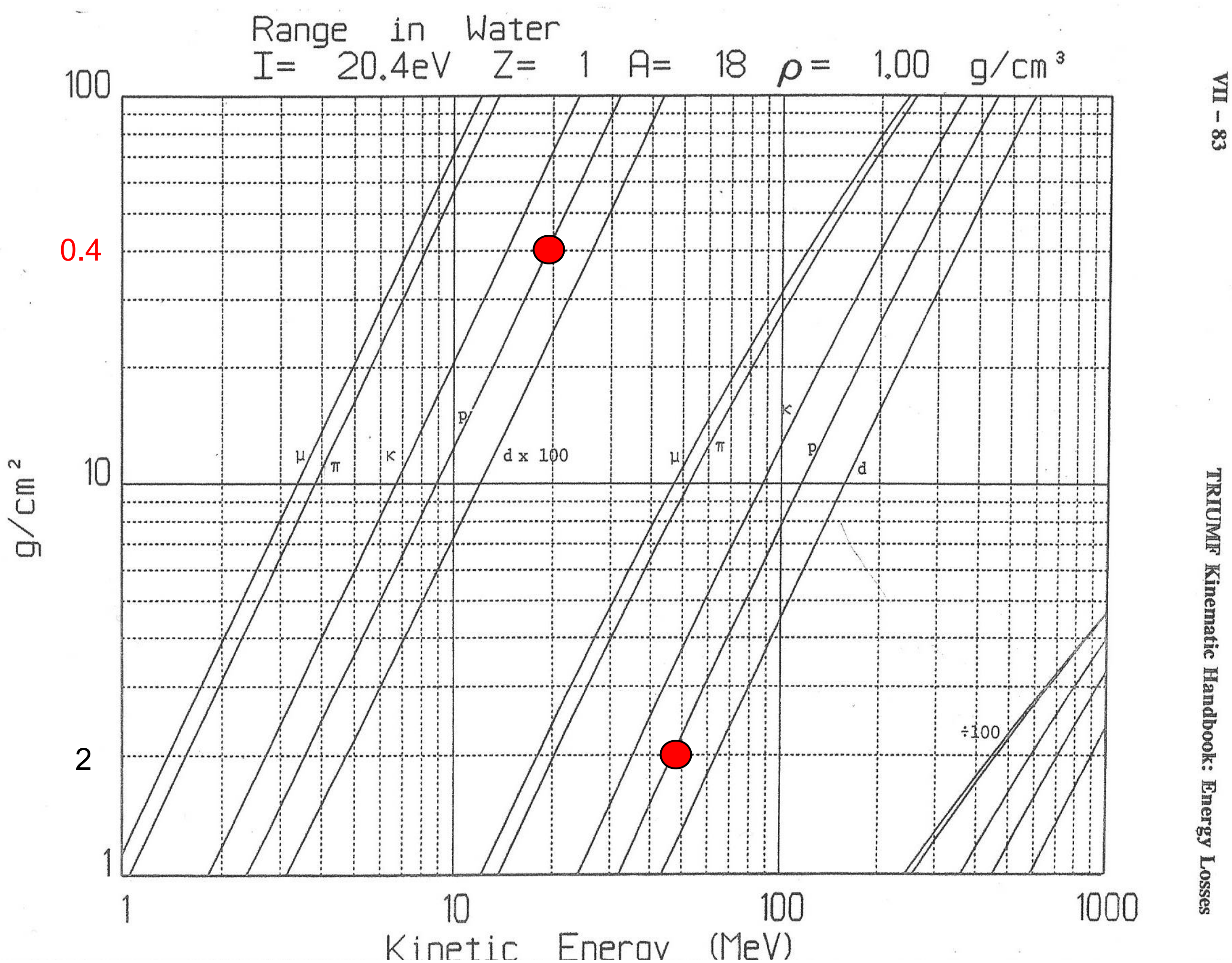

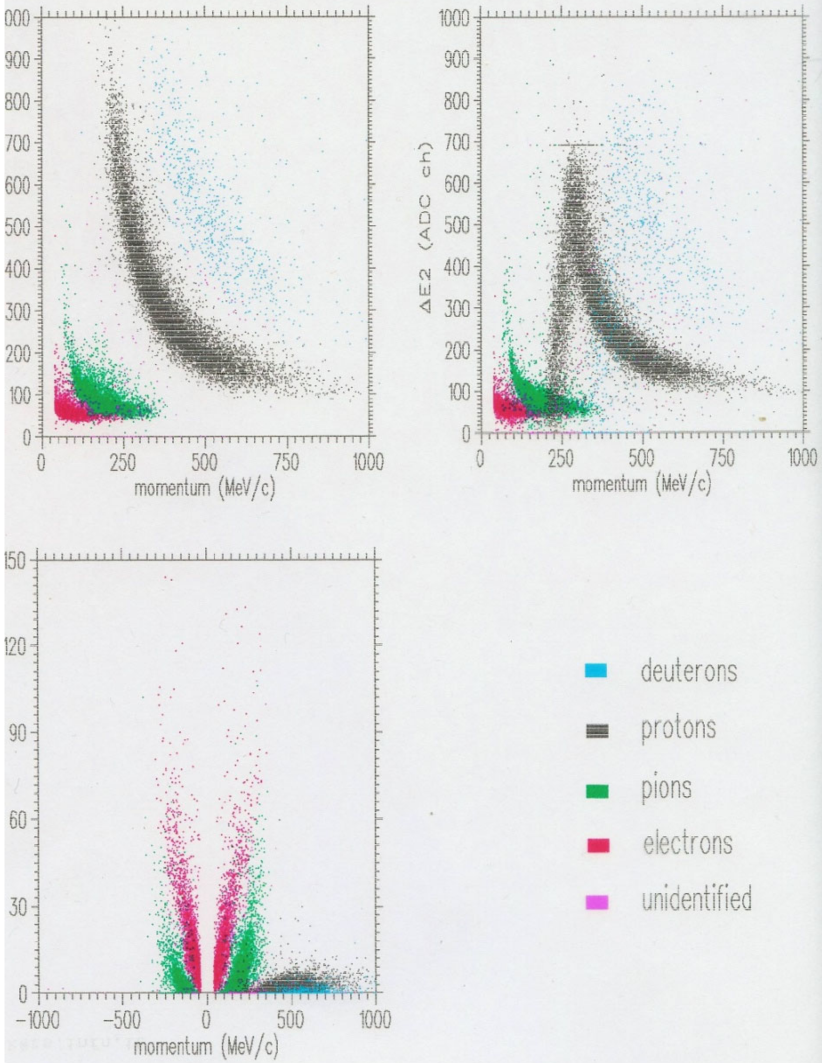
ΔE2 (ADC ch)
momentum (MeV/c)
momentum (MeV/c)
momentum (MeV/c)
deuterons
protons
pions
electrons
unidentified

Range for protons in pl. scint

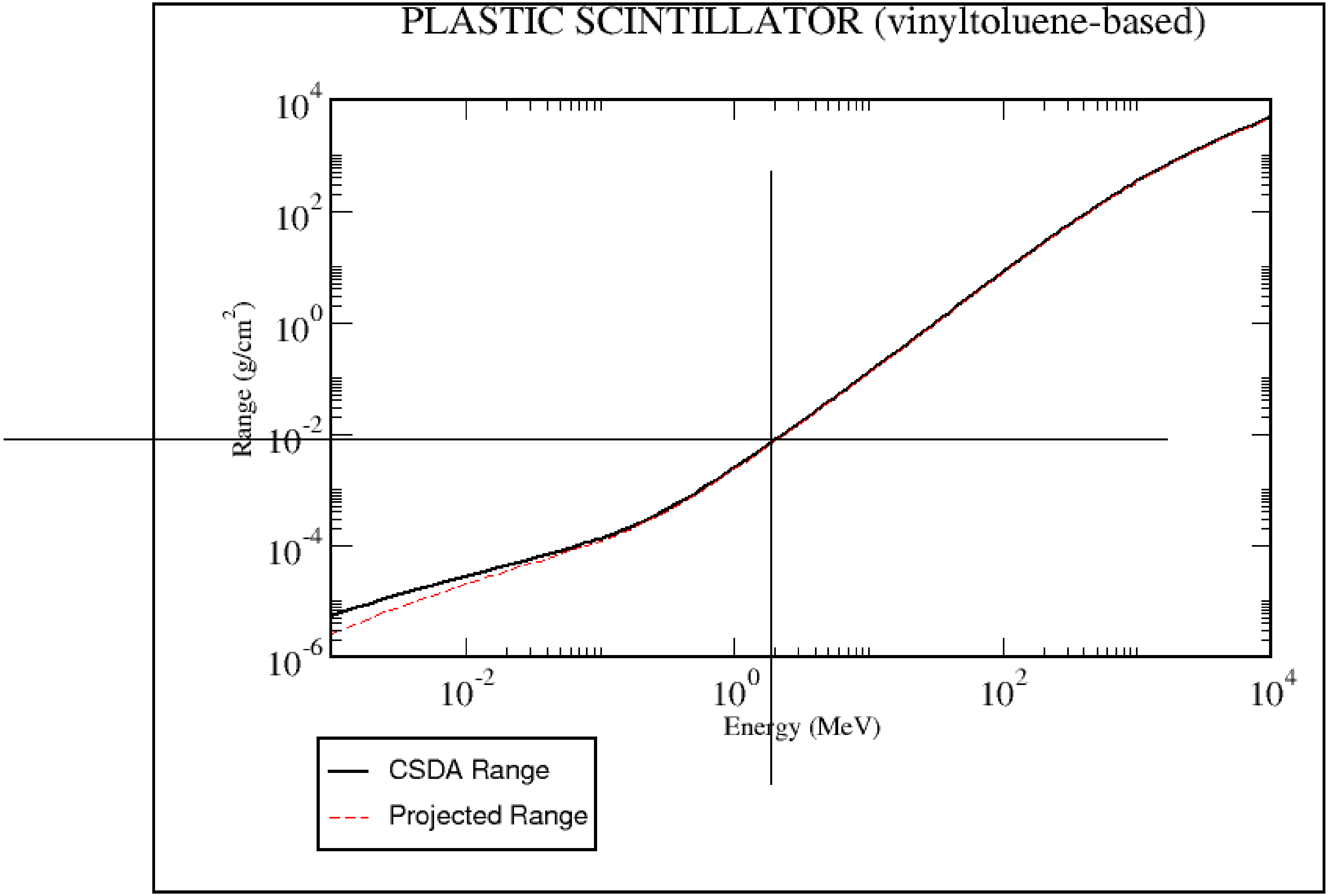

Stopping power for protons in silicon

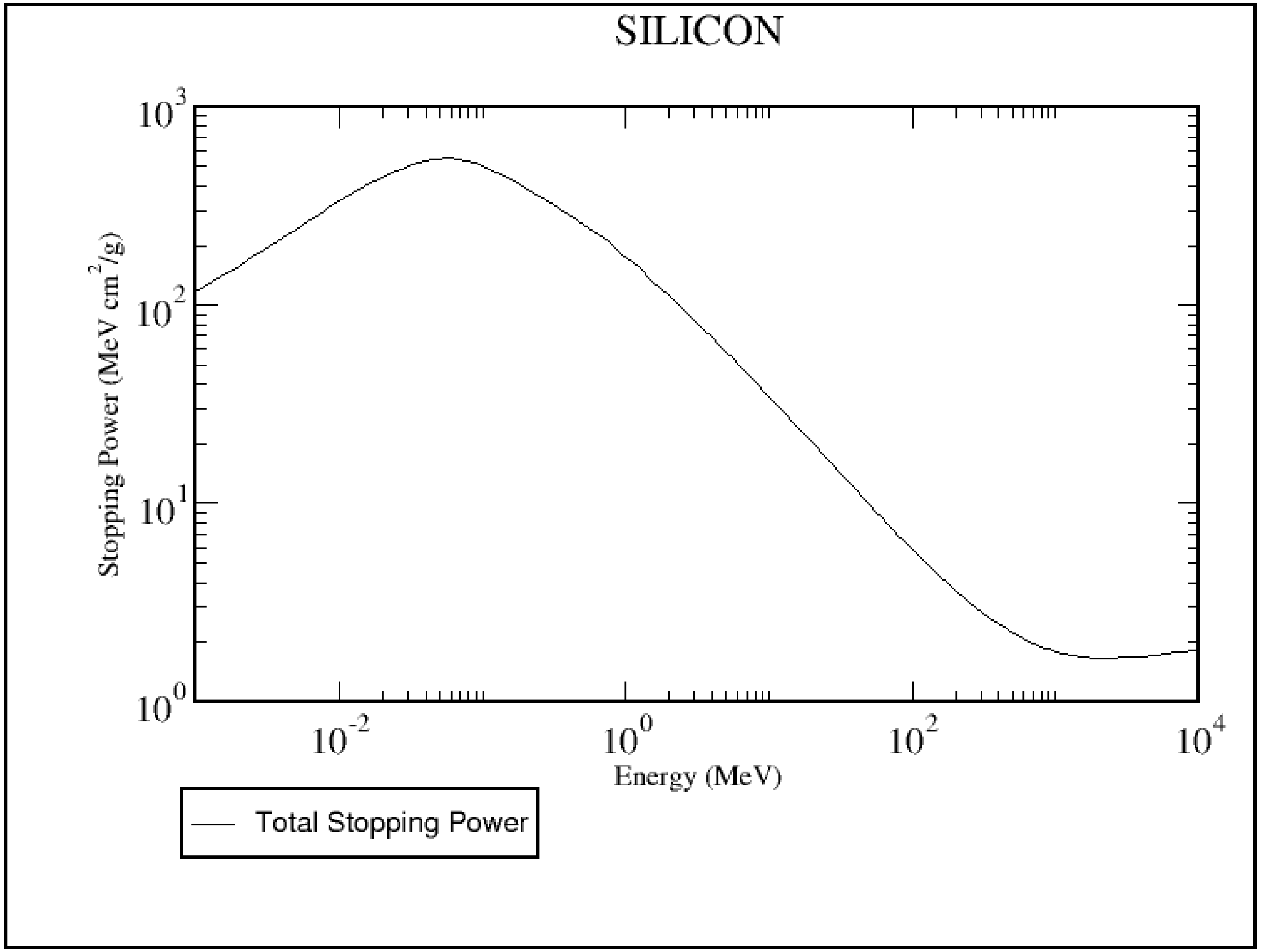

Range for protons in silicon

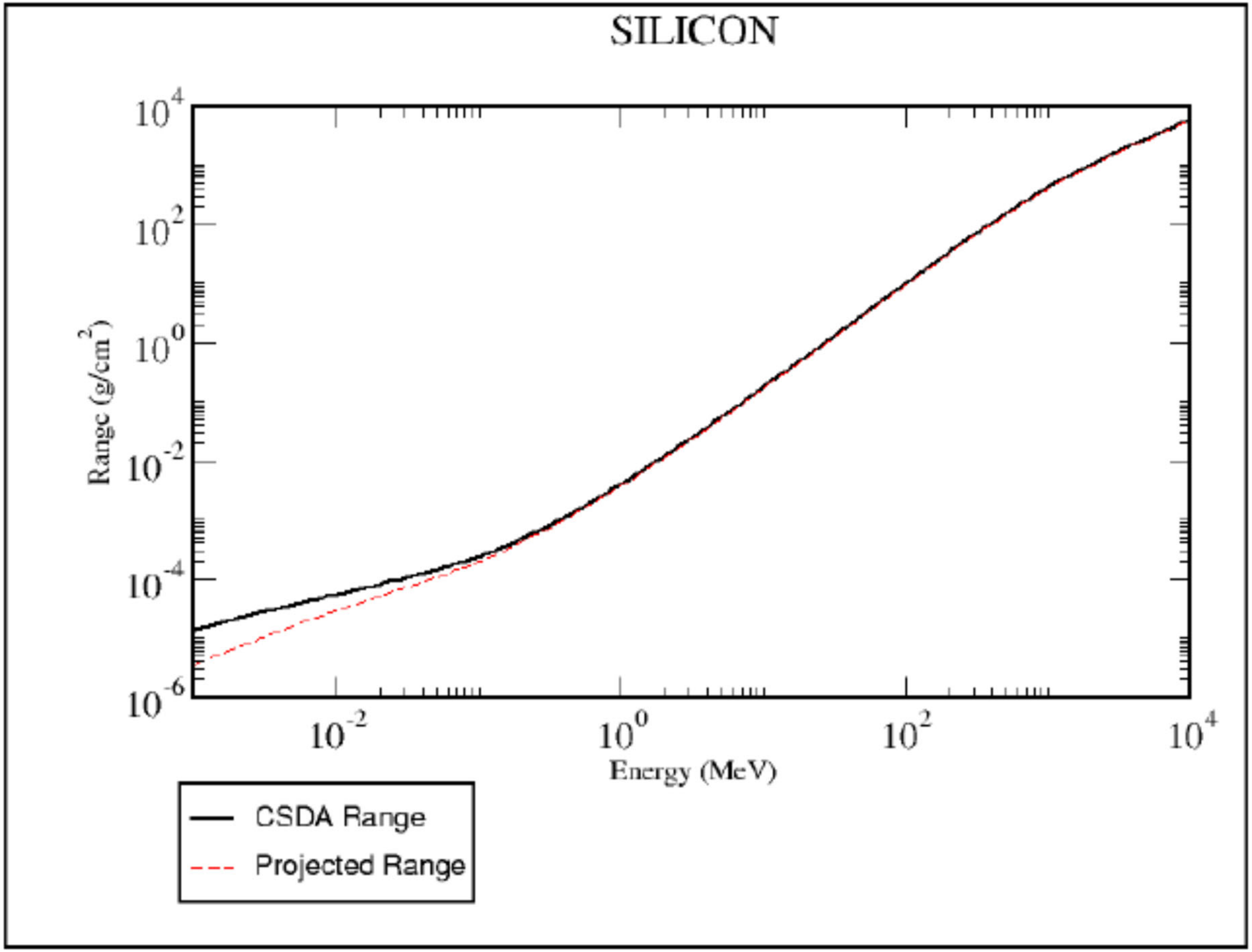

Stopping power for electrons in pl. scint

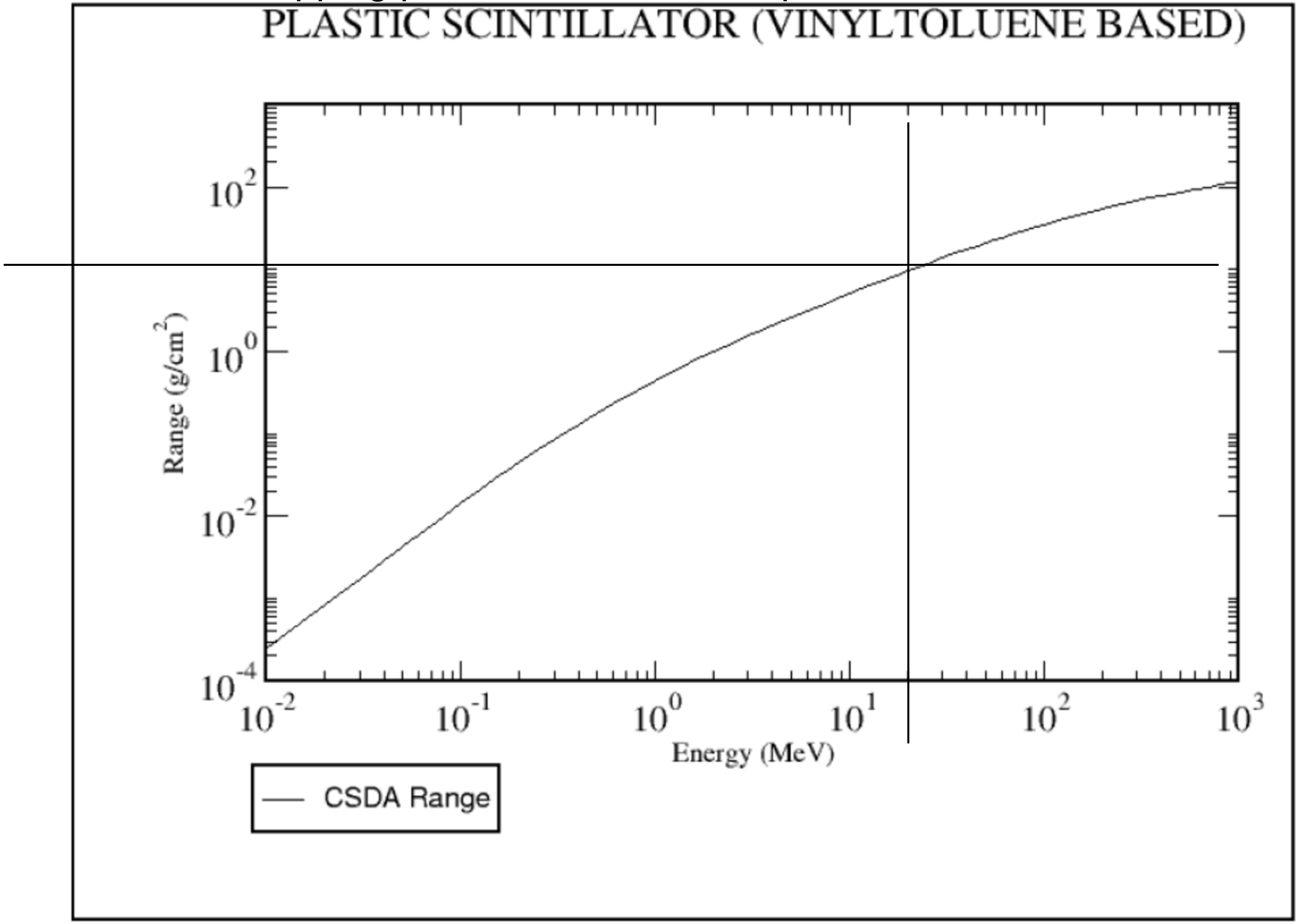

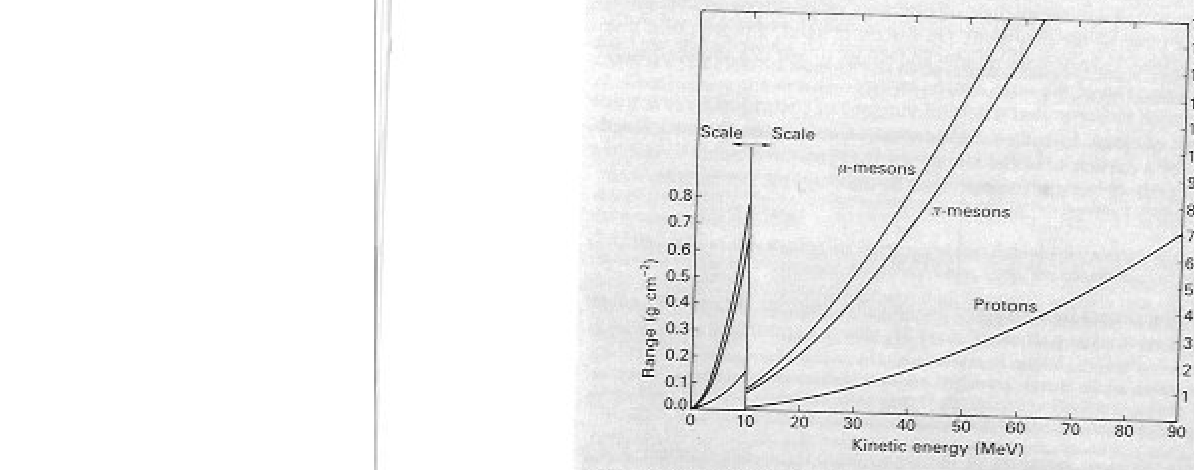

Fig. 11.3 The range–kinetic energy curves for protons, π-mesons and μ-mesons in carbon. Equation (11.1) tells us that at low energies the rate of energy loss is varying inversely as the velocity squared and therefore every increment in incident energy requires a disproportionate increase in range to remove that increase in energy; thus for all particles the range increases faster than linearly with the incident kinetic energy. In addition, Figure 11.2 shows that for the same kinetic energy lighter particles suffer less energy loss and therefore have greater ranges. Thus the features of this figure can be predicted from the properties of the stopping power.

the two particles. Light electrons of a given velocity have low momentum and are easily scattered or badly suffer the effect of multiple scattering, both of which cause an increasing deviation from a straight track, and that means that the track length has a projection on the original electron direction which is shorter or much shorter than the track length (see Fig. 11.5). For α-particles of the same velocity, the momentum is much greater and the track suffers much less deviation and the projected track length is in most cases only slightly less

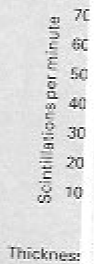

Fig. 11.4 The transı
hydrogen gas at 15°
other curves by visu
from a source reach
scintillations per mir
energy the chance o
the loss of energy
fluctuation on the n
α-particles travel the
until a thickness cl
definition of range is
and the fact that the
length (Fig. 11.5). I
range could be cu
scintillations become
point where the cur
Fig. 6.6 is a cloud
unique range and sn

angle deviation is ap
deviation, θ_0; it is th

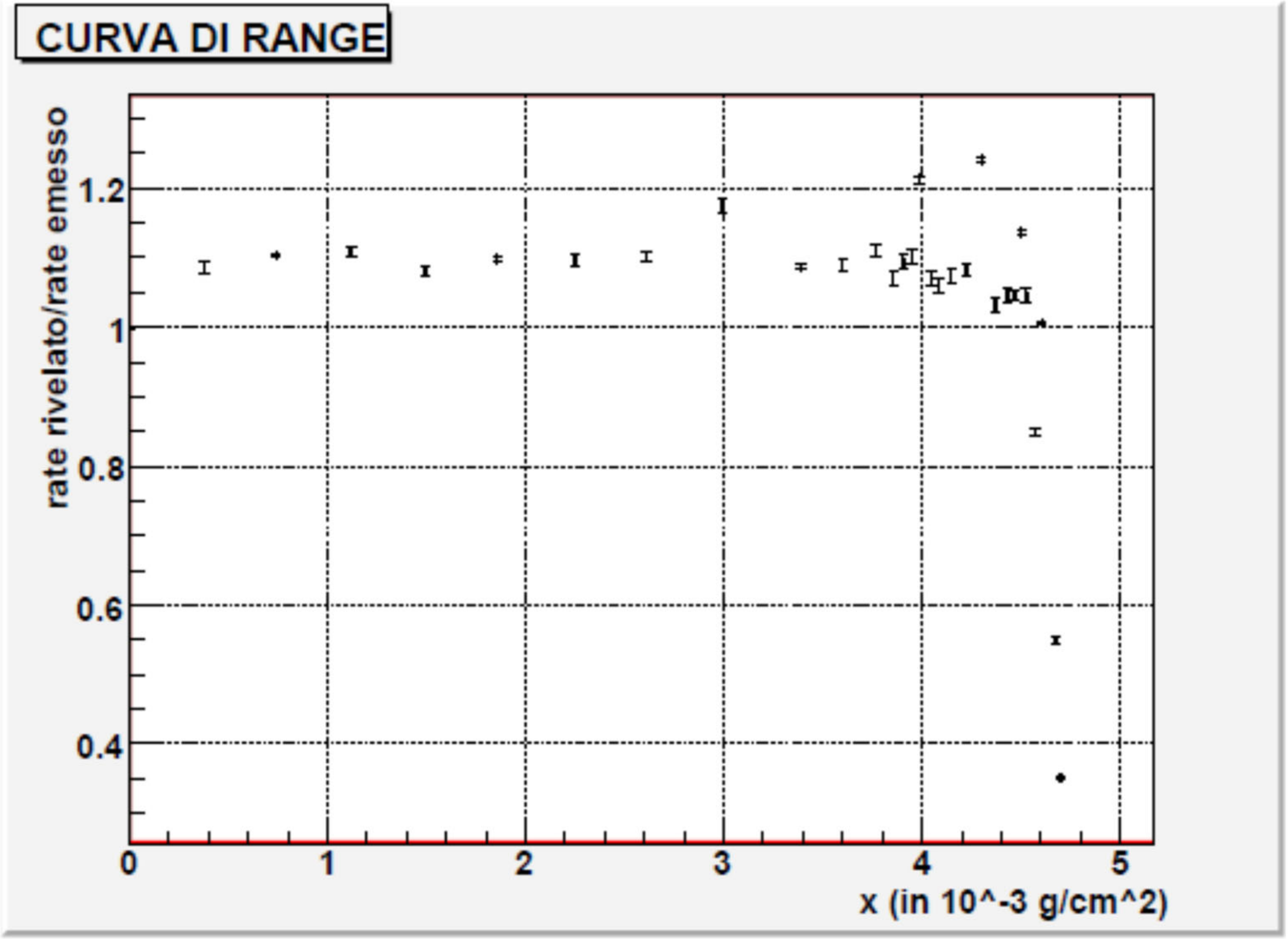

Curva di range sperimentale.

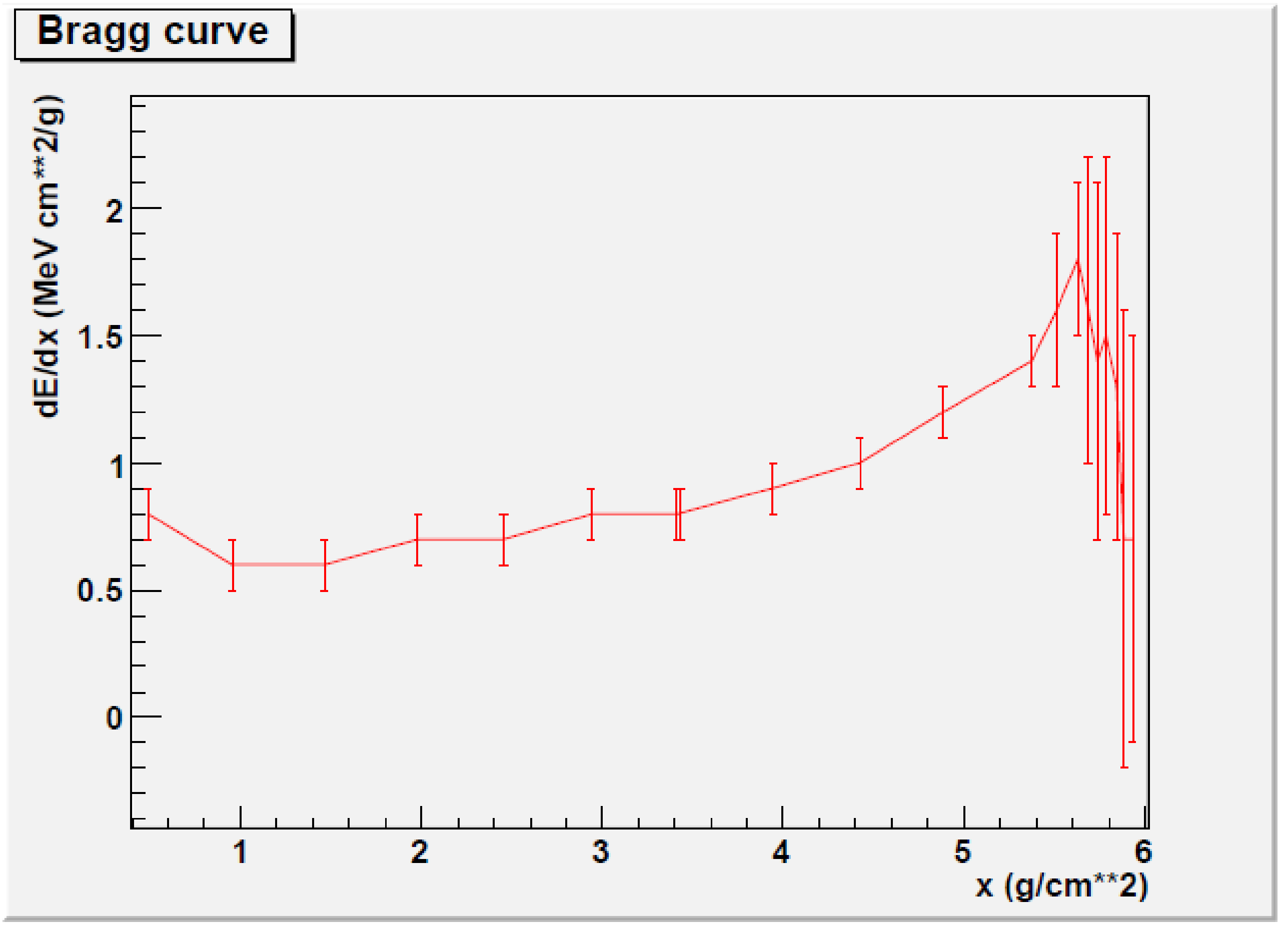

Figura 8: Grafico della curva di Bragg.

235 MeV Proton Bragg Curve

Loma Linda University Medical Center

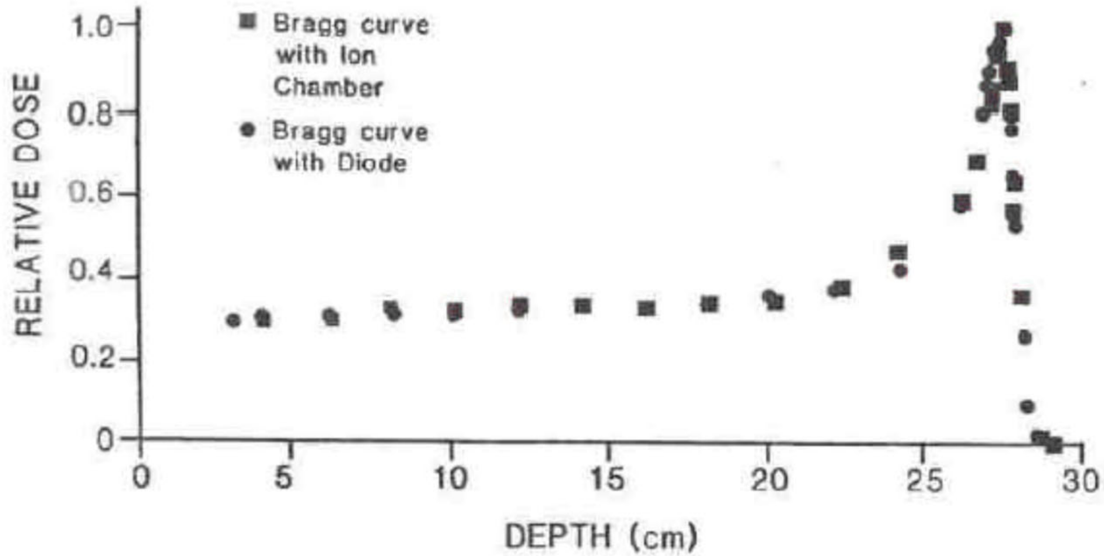

- Suitable for 1.5 cm diameter tumor.
- Skin dose ~30% of maximum dose.

Coutrakon *et al*, Med. Phys.1991. 18:1093-1099.

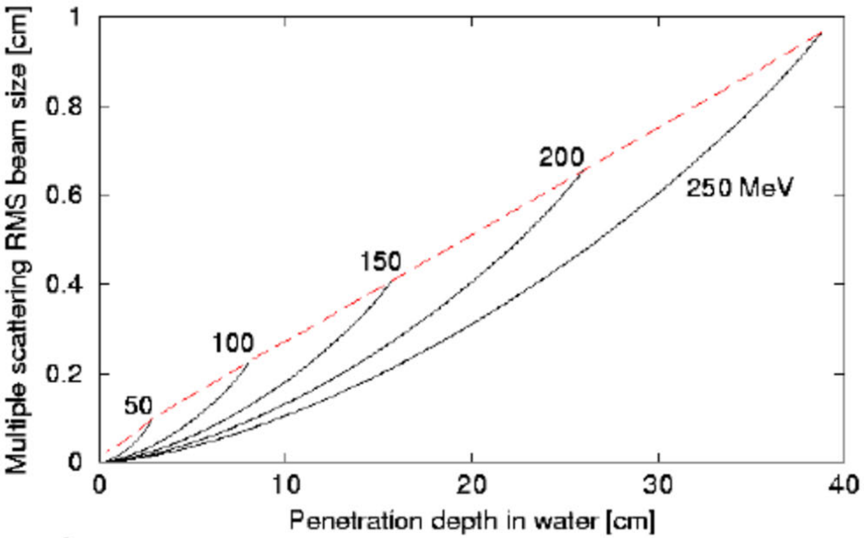

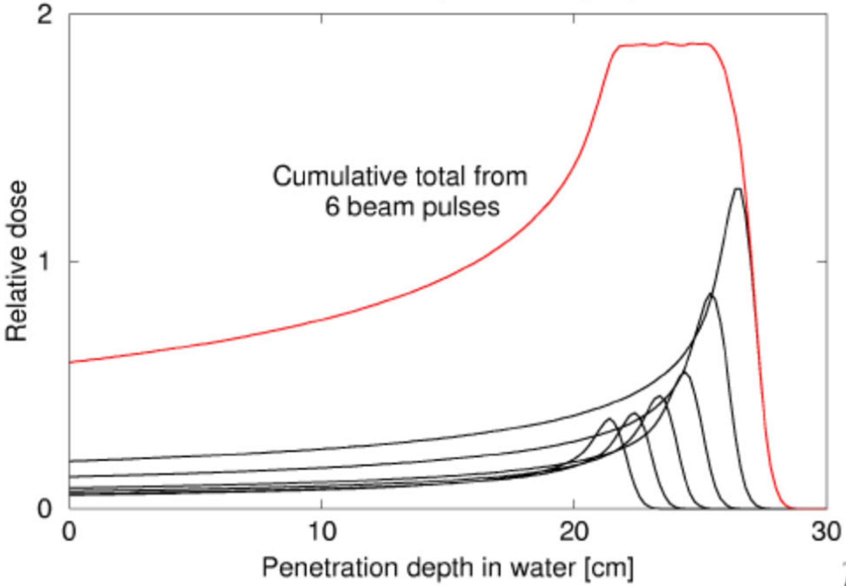

A perfect monochromatic proton beam, with zero initial emittance:

TOP spreads out transversely

BOTTOM acquires an energy spread that blurs the Bragg peak

Steer the beam and modulate its energy to "paint" the tumor!

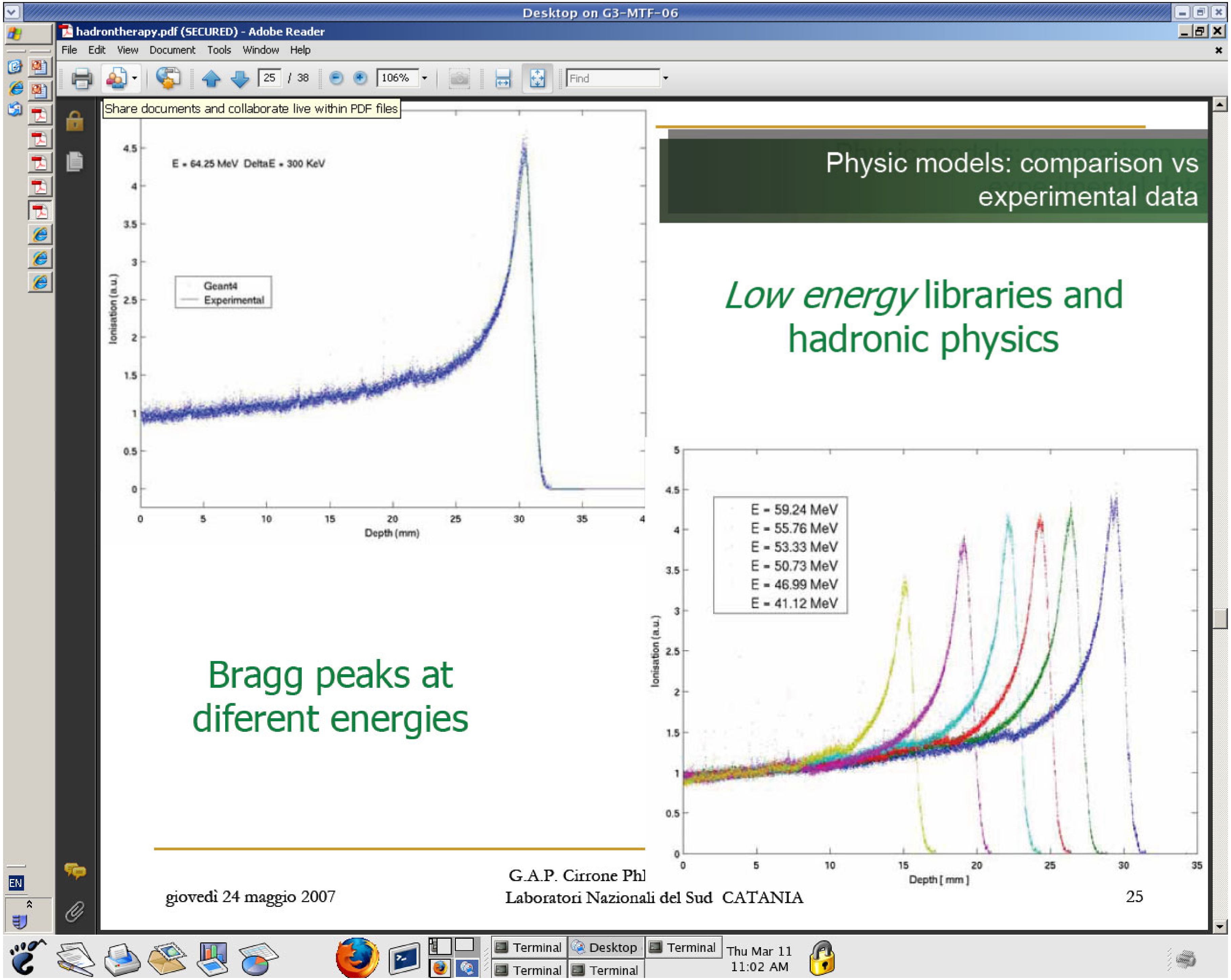
Desktop on G3-MTF-06
hadrontherapy.pdf (SECURED) - Adobe Reader
File Edit View Document Tools Window Help
25 / 38
106%
Find
Share documents and collaborate live within PDF files
E = 64.25 MeV DeltaE = 300 KeV
Geant4
Experimental
Ionisation (a.u.)
Depth (mm)
Physic models: comparison vs experimental data
Low energy libraries and hadronic physics
E = 59.24 MeV
E = 55.76 MeV
E = 53.33 MeV
E = 50.73 MeV
E = 46.99 MeV
E = 41.12 MeV
Ionisation (a.u.)
Depth [mm]
Bragg peaks at diferent energies
G.A.P. Cirrone PhI
giovedì 24 maggio 2007
Laboratori Nazionali del Sud CATANIA
25
Terminal
Desktop
Terminal
Terminal
Terminal
Thu Mar 11
11:02 AM
EN

Energy straggling. Thin absorbers

Horst, fontana, basilico, hansel adams

Interaction of charged particles

Real detector (limited granularity) can not measure <*dE/dx*> !

It measures the energy ΔE deposited in a layer of finite thickness δx.

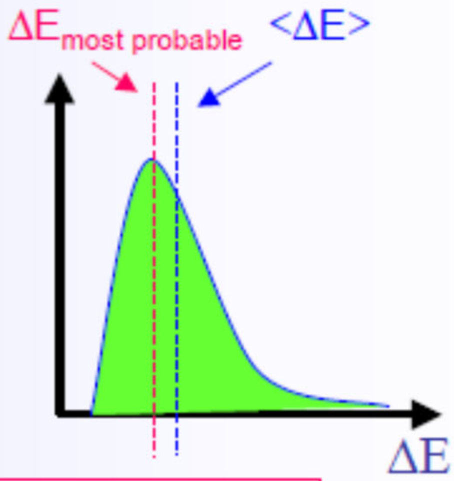

For thin layers or low density materials:

→ Few collisions, some with high energy transfer.

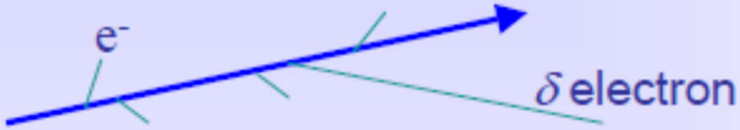

→ Energy loss distributions show large fluctuations towards high losses: "Landau tails"

Example: Si sensor: 300 μm thick. $\Delta E_{m.p} \sim 82$ keV $\quad <\Delta E> \sim 115$ keV

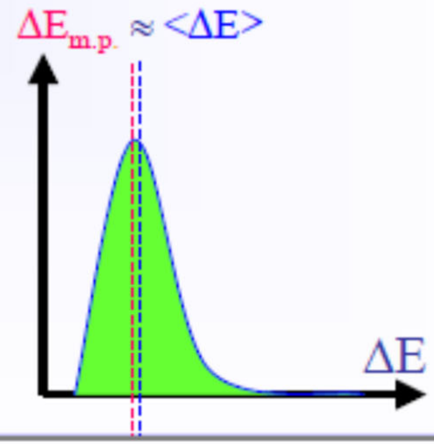

For thick layers and high density materials:

→ Many collisions.
→ Central Limit Theorem → Gaussian shaped distributions.

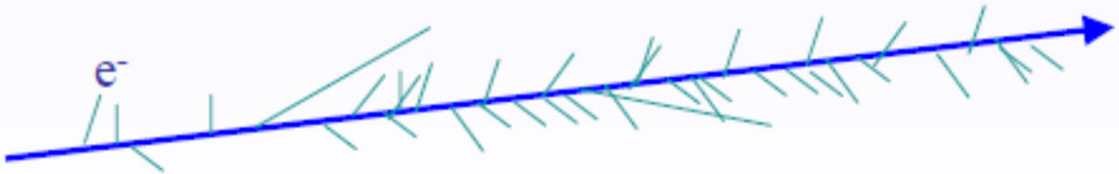

Interaction of charged particles

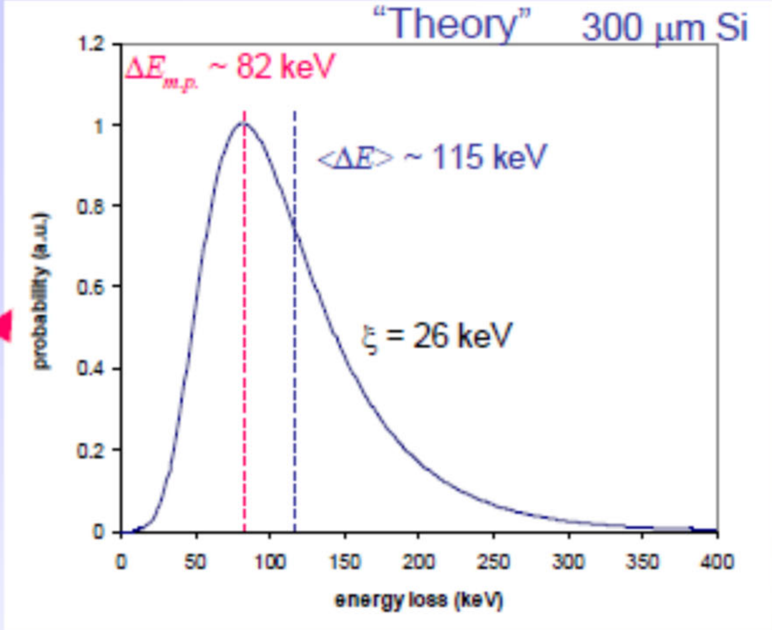

Landau's theory J. Phys (USSR) 8, 201 (1944)

$$f(x,\Delta E) = \frac{1}{\xi}\Omega(\lambda) \qquad \Omega(\lambda) \approx \frac{1}{\sqrt{2\pi}}\exp\left\{-\tfrac{1}{2}(\lambda + e^{-\lambda})\right\}$$

$$\lambda = \frac{\Delta E - \Delta E_{m.p.}}{\xi}$$

$$\xi = \frac{2\pi N e^4}{m_e v^2}\frac{Z}{A}x$$

x (300 μm Si) = 69 mg/cm^2

charge collection is not 100%

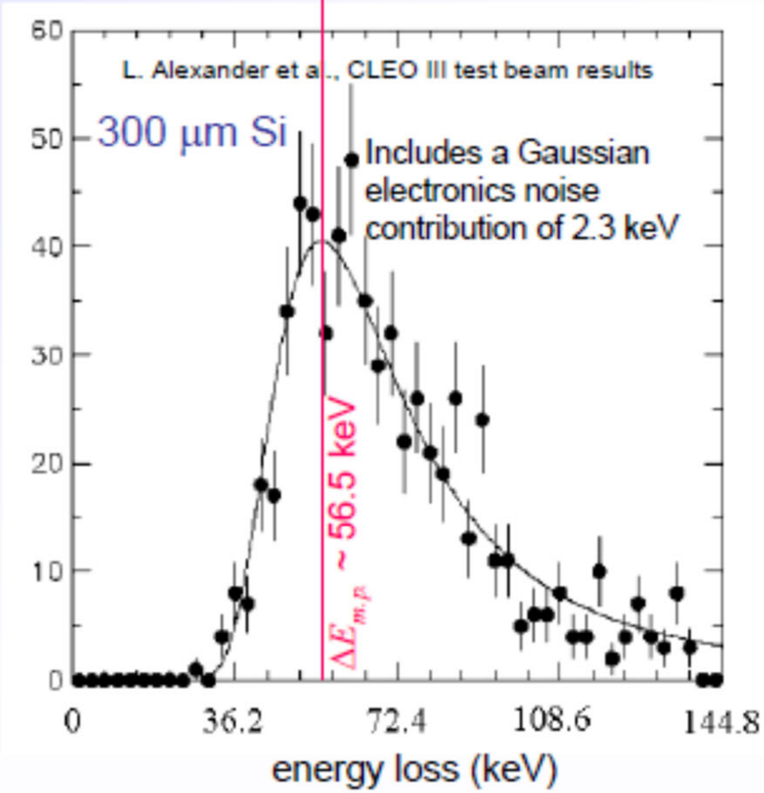

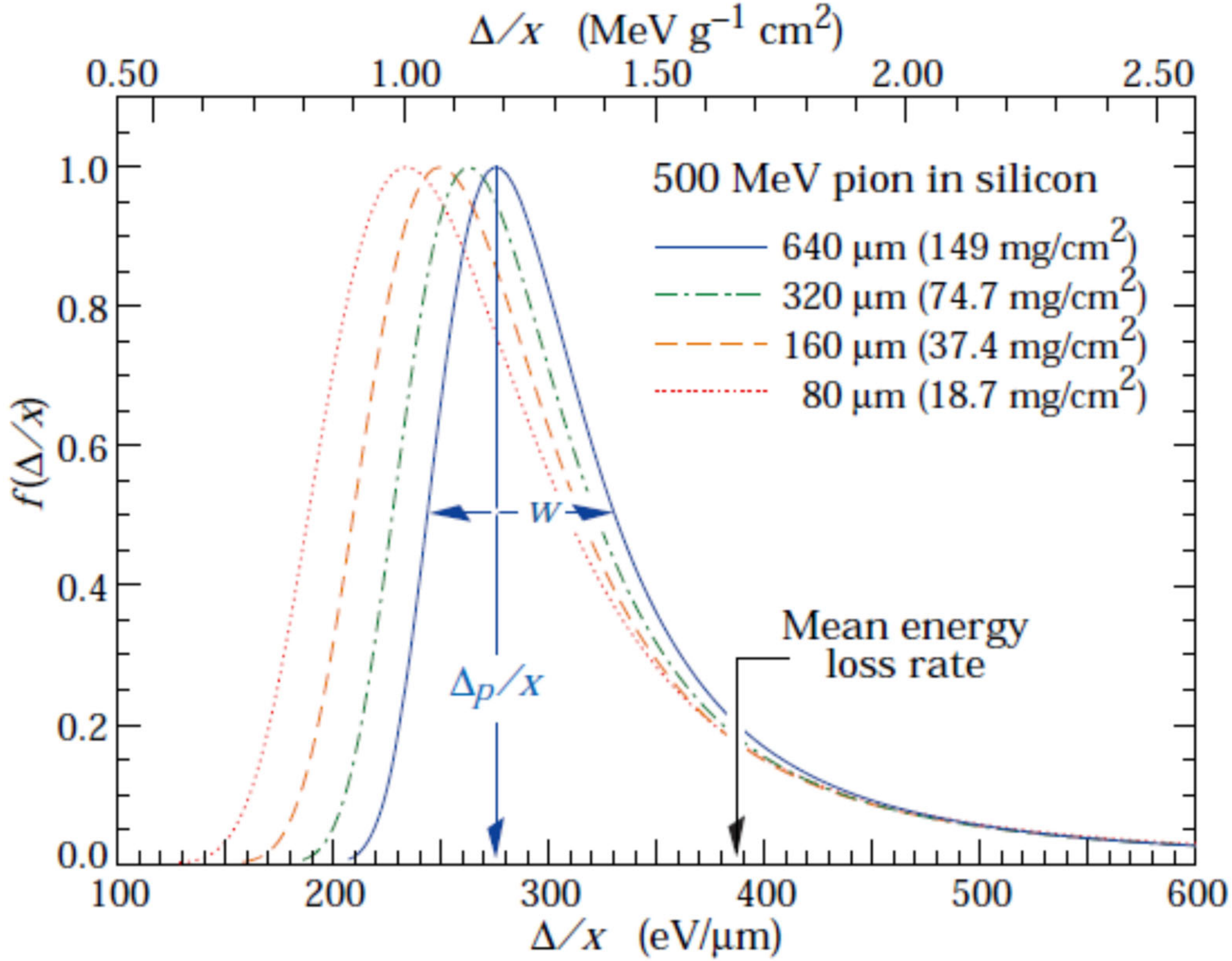

Figure 27.7: Straggling functions in silicon for 500 MeV pions, normalized to unity at the most probable value δ_p/x. The width w is the full width at half maximum.

fluttuazioni che sono descritte dalla distribuzione

Landau :

$$L(\lambda)=\frac{1}{(\sqrt{(2\pi)})}\exp(\frac{-1}{2}(\lambda+e^{(-\lambda)}))$$

- $$\lambda=\frac{(\Delta E-\Delta E_m)}{(\zeta)}$$

- $$\zeta=2\pi N_0 r_e^2 m_e z^2 c^2 \frac{Z}{A}\frac{1}{(\beta^2)}\rho x$$

La grande fluttuazione nella perdita di energia tra un evento ed un alt

condiziona la risoluzione energetica dei rivelatori sottili .

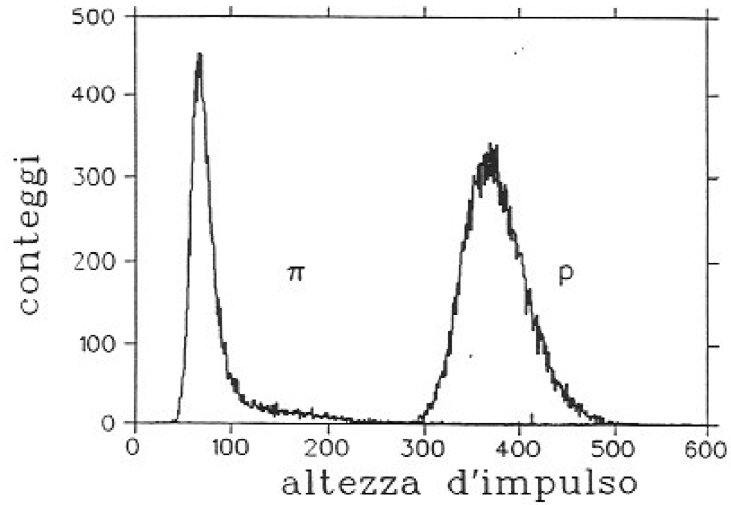

Fig.5.6- Altezza d'impulso di π^+, p in $\Delta E1$ per p=400 MeV/c.

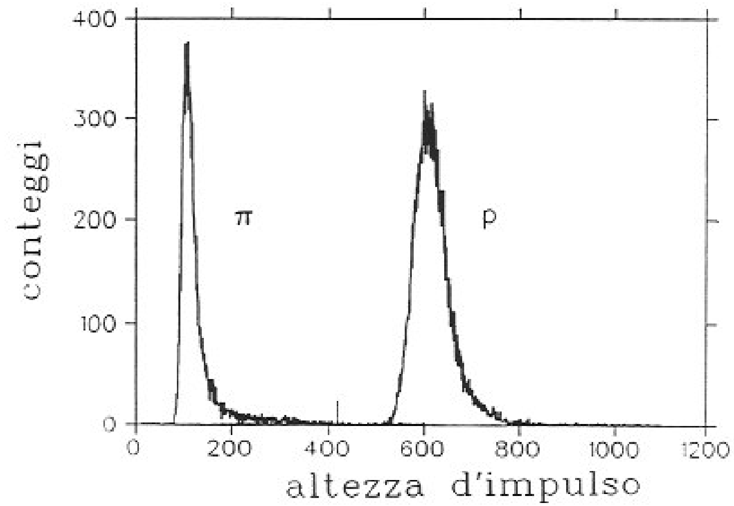

Fig.5.7- Altezza d'impulso di π^+, p in $\Delta E2$ per p=400 MeV/c.

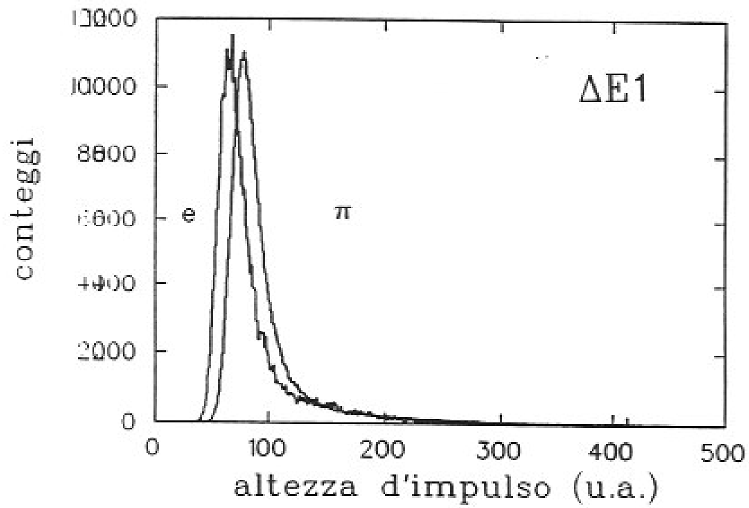

Fig.5.10- Altezza d'impulso di e^+ π^+ in ΔE1 per p=240 MeV/c.

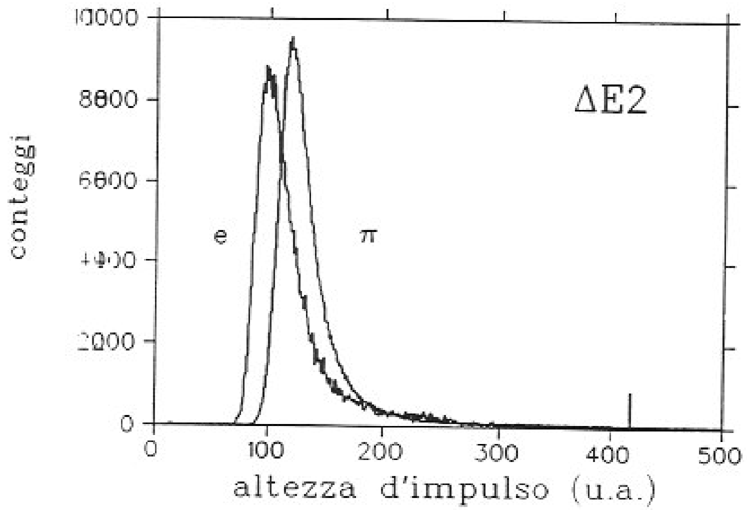

Fig.5.11- Altezza d'impulso di e^+ π^+ in ΔE2 per p=240 MeV/c.

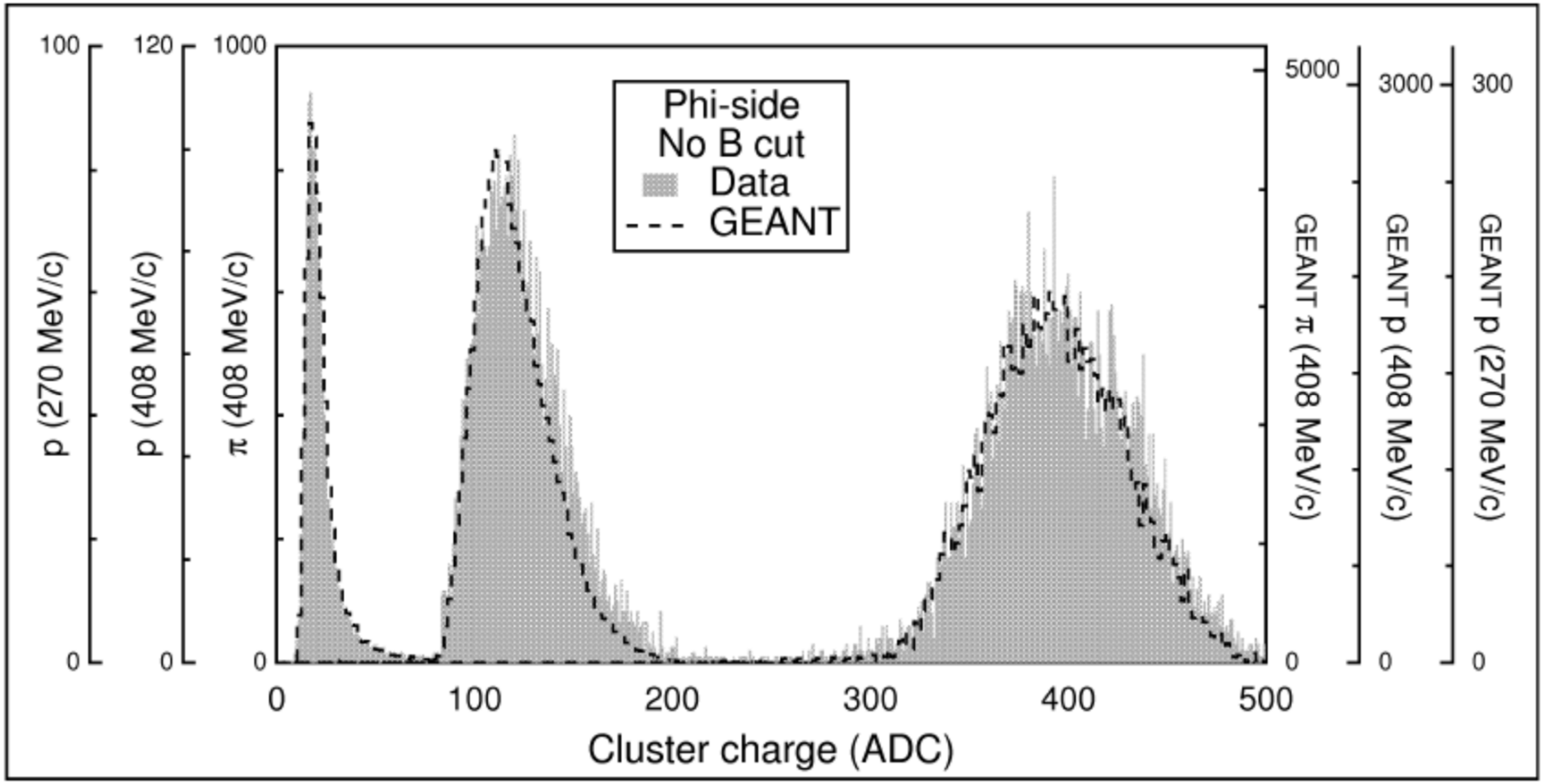

Phi-side
No B cut
Data
GEANT
p (270 MeV/c)
p (408 MeV/c)
π (408 MeV/c)
GEANT π (408 MeV/c)
GEANT p (408 MeV/c)
GEANT p (270 MeV/c)
Cluster charge (ADC)

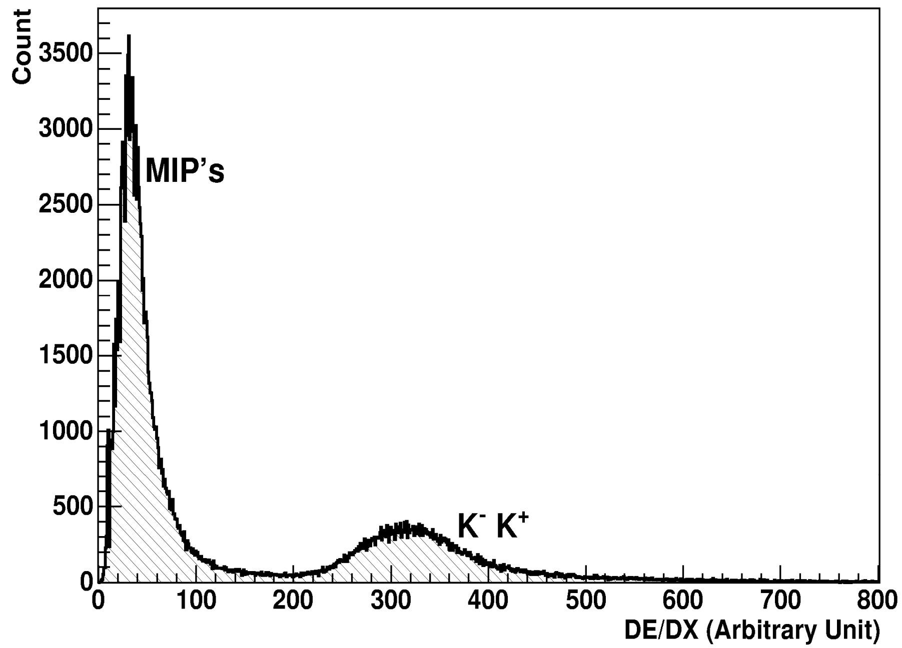

Count
3500
3000
2500
2000
1500
1000
500
0
MIP's
K- K+
0
100
200
300
400
500
600
700
800
DE/DX (Arbitrary Unit)

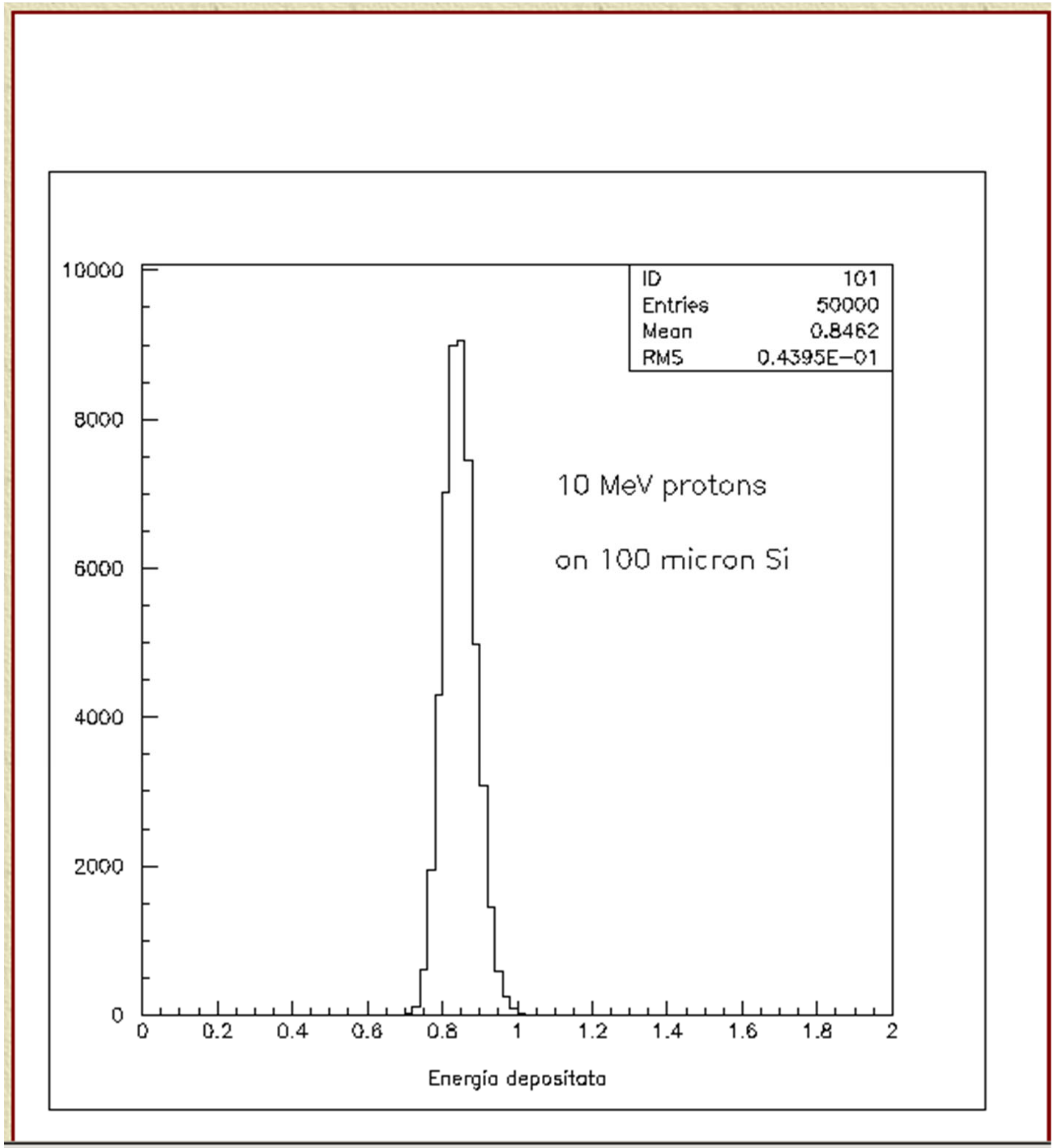

ID 101
Entries 50000
Mean 0.8462
RMS 0.4395E-01
10 MeV protons
on 100 micron Si
10000
8000
6000
4000
2000
0
0.2
0.4
0.6
0.8
1
1.2
1.4
1.6
1.8
2
Energia depositata

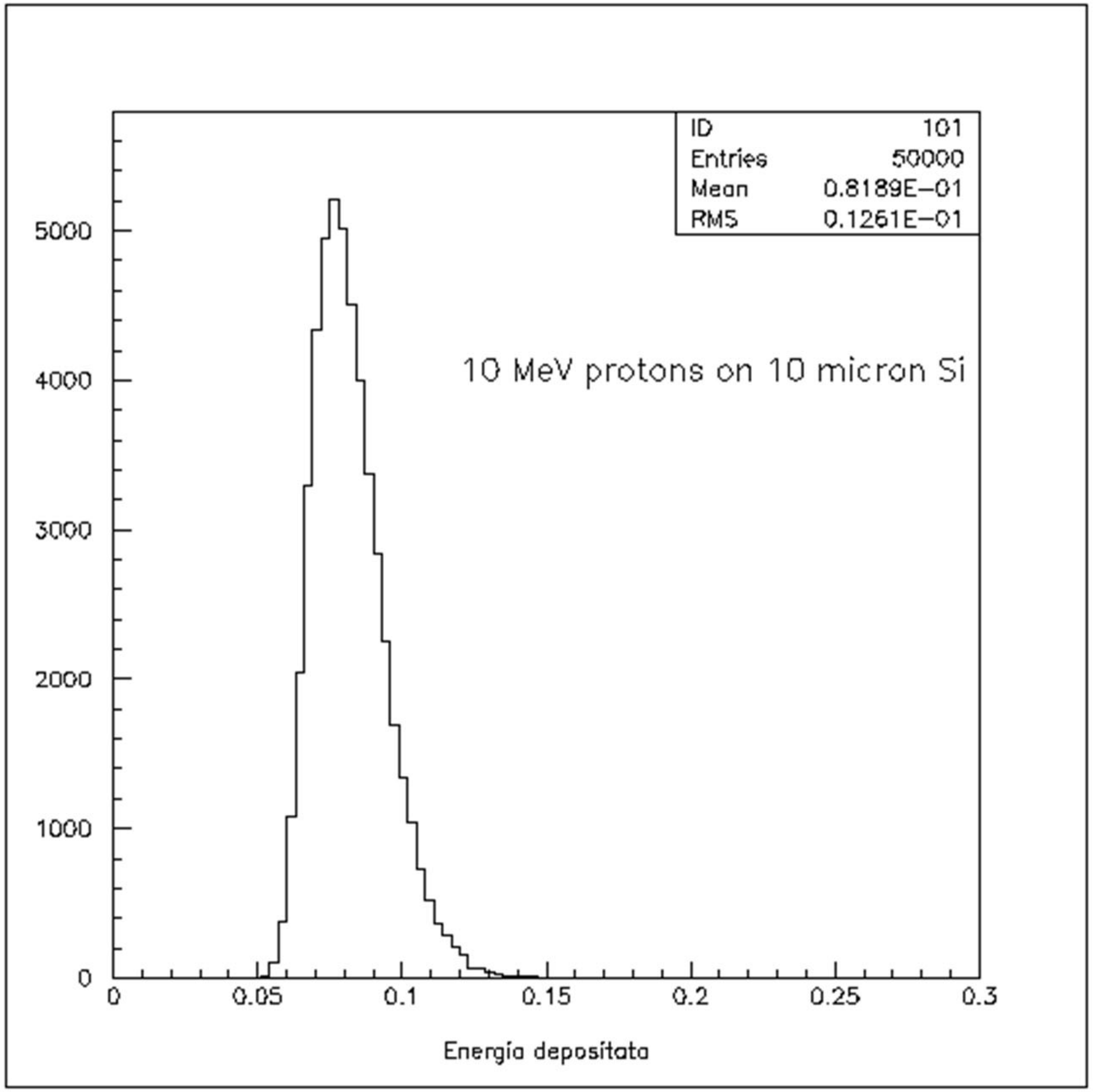
ID 101
Entries 50000
Mean 0.8189E-01
RMS 0.1261E-01
10 MeV protons on 10 micron Si
5000
4000
3000
2000
1000
0
0
0.05
0.1
0.15
0.2
0.25
0.3
Energia depositata

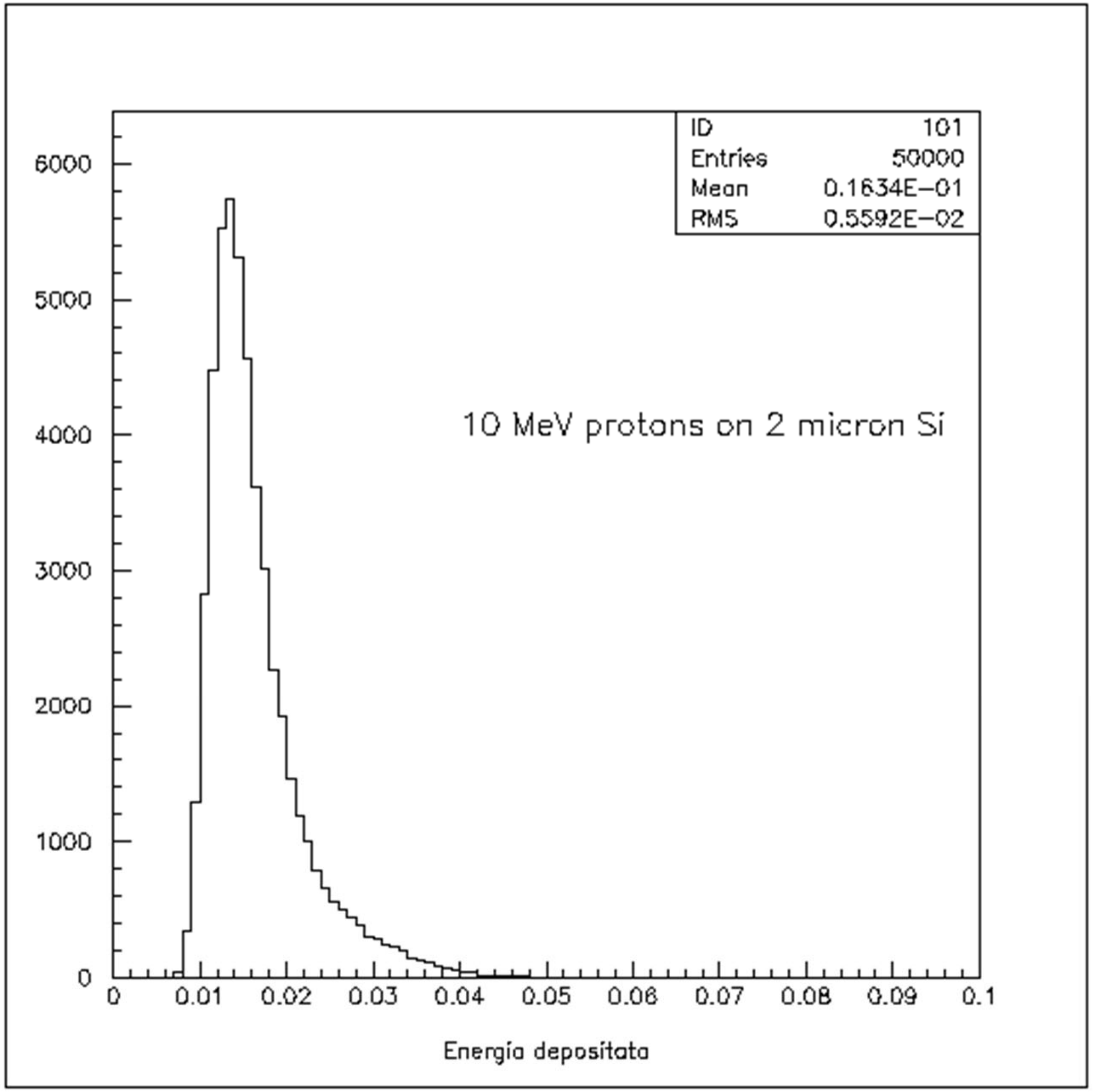

ID 101
Entries 50000
Mean 0.1634E-01
RMS 0.5592E-02
10 MeV protons on 2 micron Si
6000
5000
4000
3000
2000
1000
0
0 0.01 0.02 0.03 0.04 0.05 0.06 0.07 0.08 0.09 0.1
Energia depositata

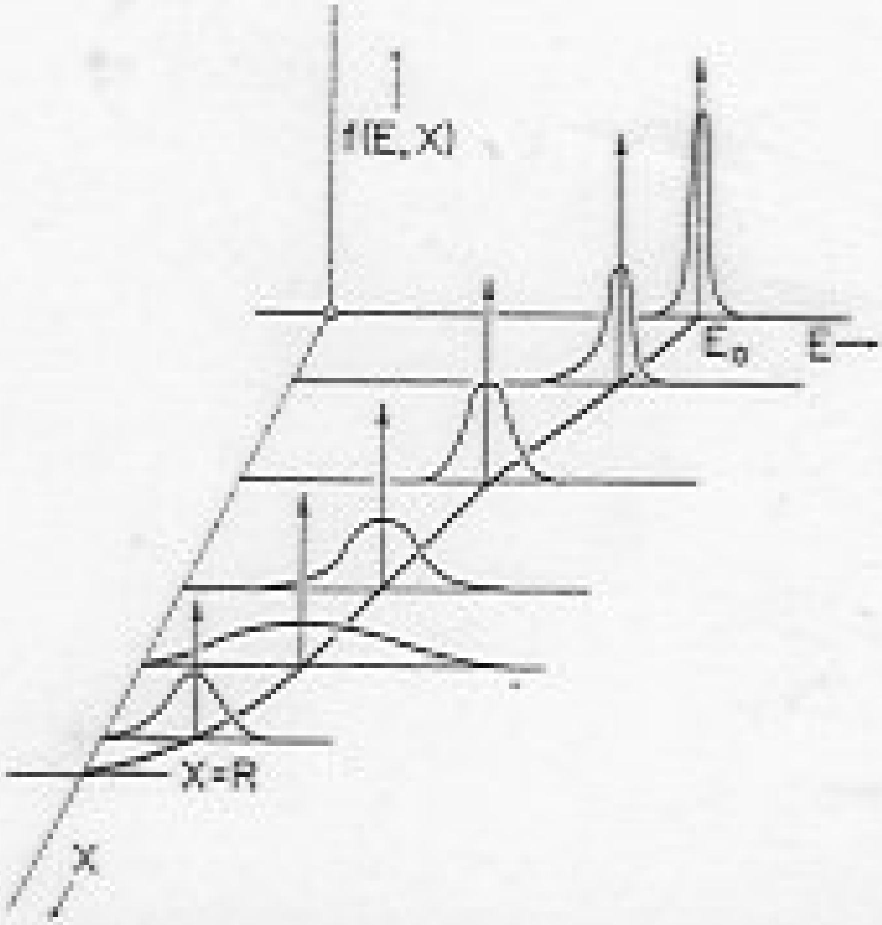

Figure 2.4 Plots of energy distribution of a beam of initially monoenergetic charged particles at various penetration distances. E is the particle energy and X is the distance along the track. (From Wilken and Fritz.[3])